PERGAMON

International Journal of Heat and Mass Transfer 45 (2002) 3299–3312

International Journal of HEAT and MASS TRANSFER

www.elsevier.com/locate/ijhmt

Tree-shaped flow structures designed by minimizing path lengths

S. Lorente [a], W. Wechsatol [b], A. Bejan [b,*]

[a] Department of Civil Engineering, National Institute of Applied Sciences (INSA), 135 Avenue de Rangueil, Toulouse 31077, France
[b] Department of Mechanical Engineering and Materials Science, Duke University, Box 90300, Durham, NC 27708-0300, USA

Received 2 November 2001; received in revised form 25 January 2002

Abstract

This paper outlines a direct route to the construction of effective tree-shaped flow structures. Dendritic flow structures dominate the design of natural and engineered flow systems, especially in thermal and fluid systems. The starting point is the optimization of the shape of each elemental area or volume, such that the length of the flow path housed by the element is minimized. Proceeding toward larger and more complex structures – from elements, to first constructs, second constructs, etc. – the paper develops tree-shaped flow structures between one point and a straight line, one point and a plane, a circle and its center, and a point and many points distributed uniformly over an area. In the latter, the construction method is applied to a fluid flow configuration with laminar fully developed flow. The constructions reveal several features that are supported by empirical observations of natural tree-shaped flows: asymmetry, flow rate imbalance, pairing or bifurcation, angles between branches, and Y-shaped constructs that lie in a plane. It is shown that these basic features are necessary because of "packing", i.e., assembling optimized elements into a fixed space, and filling the space completely. For the flow between an area and one point, the best elemental shape is the regular hexagon. It is shown that the emergence of string-shaped links that connect two or more elements are necessary features, which are also required by packing. Strings cover some of the inner zones of the tree network, particularly the inner zones of large and complex trees. Dichotomous Y-shaped constructs dominate the tree structure, especially the peripheral zones of the tree canopy. The practical importance of the simplified design method is discussed.

Keywords: Constructal theory; Tree networks; Topology optimization; Dendritic; Flow geometry; Design

1. Introduction

In this paper we propose a simpler and more direct route to the construction of optimized tree-shaped paths for flows between discrete points (sources, sinks) and infinite numbers of points (lines, areas, volumes). Tree-shaped flow architectures are everywhere in nature and engineering. They are so prevalent and important that their design – the generation of optimal geometric form – recommends itself as a principle that unifies the natural flows with the engineered [1]. Many things flow along tree-shaped paths: fluids, electricity, heat, goods, people, information, etc. Reviews of the morphology of tree flows in heat transfer, microchannel networks, electronics cooling, fluids engineering, geophysics, physiology, urban design, transportation and many other sectors of engineering are provided in [1–8].

To see the simplicity of the proposed method, it is useful to review the theoretical (predictive) methods that have been used until now. The regular architectures of bronchial trees and vascularized tissues, coupled with the belief that the urge to "survive" pushes the most complex flow systems (e.g., animals) toward greater global performance ("the fittest"), have fueled the speculation that tree flows too are results of optimization. They are flow systems with objective (or purpose) and constraints (e.g., volume). Without purpose and

* Corresponding author. Tel.: +1-919-660-5309; fax: +1-919-660-8963.
E-mail address: dalford@duke.edu (A. Bejan).

0017-9310/02/$ - see front matter
PII: S0017-9310(02)00051-0

Nomenclature

a	length (m)
A_i	area (m^2)
b	distance (m), Eq. (15)
b'	distance (m), Eq. (18)
c	length (m)
c_0, c_a	dimensionless ratios, Eq. (22)
C, C'	factors, Eqs. (12) and (19)
d	elemental length (m)
D, D_i	tube diameters (m)
e, f, g, l	lengths (m)
f	global flow resistance, dimensionless, Eq. (23)
L, L_i	lengths (m)
$\dot{m}_i$	mass flow rate (kg/s)
n_0	number of tubes that reach the center
N	number of points on the circular perimeter
p	number of pairing levels
P	point on the tree periphery, Fig. 1
$\tilde{P}$	dimensionless overall flow resistances, Eqs. (14) and (20)
Q	first junction, Fig. 1
r_i	radial distance (m)
R	second junction, Fig. 1
S	third junction, Fig. 1
V_i	volume (m^3)
V_t	tube volume (m^3)
x	ratio, δ/r
$x_{1,2,3}$	relative lengths, Fig. 9(a)

Greek symbols

β	angle (rad)
γ	angle (rad)
δ_i	radial thickness (m)
ΔP	pressure drop (Pa)
θ_i	angles (rad)
λ	Lagrange multiplier
v	kinematic viscosity (m/s^2)
ϕ	angle (rad)
Φ	function, Eq. (7)

Subscripts

bent Y	bent Y-shaped construct, Fig. 2
flat Y	plane Y-shaped construct, Fig. 8
i	order of construct, assembly, complexity
k	order of link
0	elemental
$1, 2, \ldots$	first construct, second construct, ...

constraints, optimization makes no sense. All the words that are used to describe the geometric patterns that we see in nature – basic words such as survival, fittest, optimized, and best – speak of purpose and constraints, the result of which is design.

Murray [9] and several other authors [2,10] tried to predict geometrical features of tree flows from the principle of the minimization of resistance to fluid flow subject to fixed total flow volume. This principle is equivalent to the minimization of pumping power (or entropy generation, or exergy destruction) when the flow rate is specified. It is the same principle that governs the thermodynamic optimization work that goes on in many sectors of engineering. He showed that if the flow regime is laminar and fully developed in every tube of the fluid tree, and if *two* tubes come together into a single one (pairing, or bifurcation), then the optimized structure must have a special ratio of tube diameters

$$D_{i+1}/D_i = 2^{1/3}, \tag{1}$$

where D_i is the diameter of each of the two streams that flow together into or out of the tube of diameter D_{i+1}. If the flow regime is fully developed and turbulent, the optimal tube diameter ratio is $D_{i+1}/D_i = 2^{3/7}$ [1,11].

The optimal ratio of tube diameters enjoys great generality. It is independent of the lengths of the tubes. It is also independent of angles and relative orientation (layout) of the tubes. Any assumed arrangement of tubes would have to exhibit Murray's diameter ratio in order to perform best. This is why in all the subsequent theoretical work the authors focused on tube diameters, the minimization of flow resistance, and 'what else' could be optimized so that additional geometrical features of the tree could be deduced from the same resistance minimization principle. Along this route, Murray [12] showed that there exists also an optimal angle of confluence between two tubes with different diameters (i.e., with different flow resistances). The same feature was discovered in geographical economics by Lösch [13], who minimized the cost of transporting goods between two points when two modes of transportation are available (e.g., land and sea).

More recently it was shown that the ratio of tube lengths can also be optimized if the additional constraint is the total volume occupied by the tube construct [11]. A large volume can be filled with a tree-shaped flow network by assembling optimized tube constructs into progressively larger constructs. This sequence of construction (from small to large) starts from an elemental volume that has a finite size and a single tube. The shape of the elemental volume is also optimized based on flow resistance minimization [1].

The construction method proposed in the present paper differs from the post-Murray methodology in two

very basic ways. First, the optimization of tube diameters is not an issue. Instead, we focus entirely on the geometric layout of the flow path, inside the space that houses it. In this new approach the flow 'tube' is a line segment. Chief unknowns are the length and position of each segment, i.e., the unknowns that persisted long after Murray. Optimized ratios of tube diameters can be added to the tree-shaped pattern later, that is, if the purpose of the tree is to guide a fluid (e.g., Sections 5 and 6).

Second, instead of minimizing resistance to flow, we minimize only lengths – the length of each segment. We show that from this single objective results the entire tree (lengths, angles, assembly, fitting, space filling). By contrast, to use the flow resistance is to pursue a considerably more complex objective. The flow resistance depends not only on path length but also on what flows (e.g., fluid, heat, electricity), flow regime, tube diameter, cross-sectional shape, wall surface condition, and on whether the stream has a free surface as in open channel flow (e.g., Sections 5 and 6). These complications have blurred the tree design theory from the beginning. Complications require ad-hoc assumptions, which restrict the validity of the theory to a particular class of flows.

2. Tree between one point and a straight line

Consider the problem of connecting all the points of a straight line (e.g., line P) with a single point (S) situated off the line, Fig. 1. The single point may be the source of a stream (e.g., water) and the line may represent a large number of users of the water stream. We approximate the line with a sequence of equidistant points: the distance between two consecutive points is d.

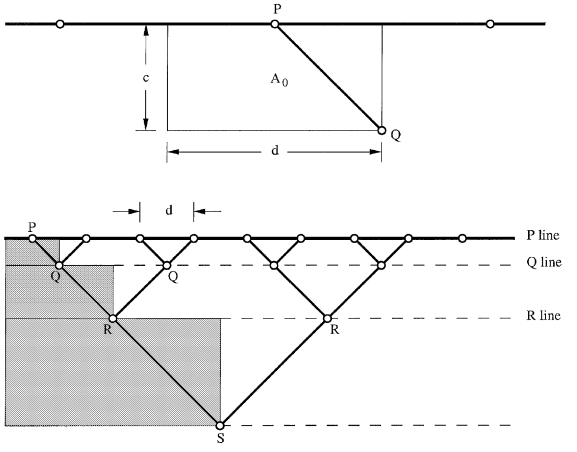

Fig. 1. Elemental system with one flow segment (top), and the construction of the minimal-length tree between a line and a point (bottom).

The space (rectangular area) around each point is finite and fixed, $A_0 = cd$, constant. This area represents the smallest element of the flow structure that will be designed. Its purpose is to allow the point (P) to communicate with the rest of the flow structure. The link is the segment PQ, where Q is a corner on the side opposite the side for which P is the midpoint (Fig. 1). An interesting feature of the elemental system is that the length of the segment PQ,

$$L_{PQ} = [(d/2)^2 + c^2]^{1/2} \tag{2}$$

can be minimized by varying the element aspect ratio c/d subject to the A_0 constraint. The PQ segment is the shortest when the aspect ratio is $c/d = 1/2$. This special shape was drawn in the upper part of Fig. 1. The link PQ makes a 45-degree angle with the line of points of type P.

Following this first optimization step, the links of type PQ occupy a strip of thickness $c = d/2$. Points of type Q occupy the lower boundary of this strip (the Q line), and the distance between them is $2d$. Each point Q is the junction of two PQ segments. Access from Q to other parts of the flow structure is effected along segments of type QR. The rectangle that houses the QR segment is completely analogous to the elemental rectangle that houses the PQ segment. These rectangles are stacked and shaded in the lower part of Fig. 1. The length of the QR segment can be minimized by selecting the aspect ratio of the rectangle that houses it. The optimal aspect ratio is the same as at the elemental level, and the minimized QR segment makes a 45-degree angle with the Q line. Eye pleasing is the coincidence that the QR segment is colinear with one of the PQ segments.

The rest of Fig. 1 outlines the subsequent steps of the construction. Each step is analogous to the preceding one, while the length scale of each optimized rectangle is the double of the preceding length scale. Two tubes are joined together at a 90-degree angle at each level of assembly. The total length from the source (point S) to each point P is the same. In other words, the tree structure generated by minimizing each segment is also the structure that maintains constant the distance between the point (S) and each of the points of line P. If we use the words 'flow resistance' instead of 'length', then the structure designed in Fig. 1 distributes uniformly the flow resistance between one point and one line. Because the resistance to flow represents the thermodynamic imperfection of the flow system, the structure derived in Fig. 1 has the merit of distributing the imperfection uniformly throughout the flow system. The optimal distribution of imperfection is a recurring feature in constructal design [1].

The tree structure may be viewed as the result of fitting together rectangular flow elements the shapes of which have been optimized. Although this 'constructal' sequence has been used before, the present construction

is new. First, contrary to the examples reviewed in [1], all the rectangular building blocks shown in Fig. 1 are geometrically similar. Second, at the elemental level the flow path PQ is not aligned with one of the sides of the elemental rectangle. Third, the present construction is not concerned with the 'diffusion' flow that would occupy the white regions of the A_0 area in order to connect Q with the infinity of points of the side on which P is situated. The entire tree architecture of Fig. 1 is a consequence of the geometric property documented by minimizing L_{PQ}.

3. Tree between one point and a plane

Consider next the three-dimensional counterpart of the construction that we just made. The problem is to connect with paths of minimum length one point to the infinity of points of a plane. We approximate the latter with a patchwork of square area elements of side d, centered at one discrete point (P). In other words, the area $d \times d$ is represented by one point in the plane. The elemental volume is fixed, $V_0 = cd^2$, constant. The connection between P and the rest of the flow structure is made along the segment PQ, where Q is the middle of one of the sides of the square situated at the distance c relative to the plane of P. The length of the PQ segment is the same as in Eq. (2), for which d and c are defined in Fig. 2. This length is minimal when the aspect ratio of the parallelepiped $d \times d \times c$ is $c/d = 2^{-3/2}$. This aspect ratio was drawn to scale in the elemental volumes shown at the top of Fig. 2.

The next volume to be optimized is $2d \times d \times e$. The link QR is from the top rectangular face (plane Q) to the middle of one of the $2d$-long sides in plane R. The length QR is minimal when the volume aspect ratio is $e/d = 2^{-3/2}$. This aspect ratio is the same as at the smallest scale.

In summary, after two steps of volume shape optimization we have covered a total volume of size $2d \times 2d \times (c + e)$. The shape of this volume is the same as that of the elemental volume, $(c + e)/2d = c/d = 2^{-3/2}$. Point R, which is the center of the bottom $(2d \times 2d)$ square is analogous to point P (the center of square

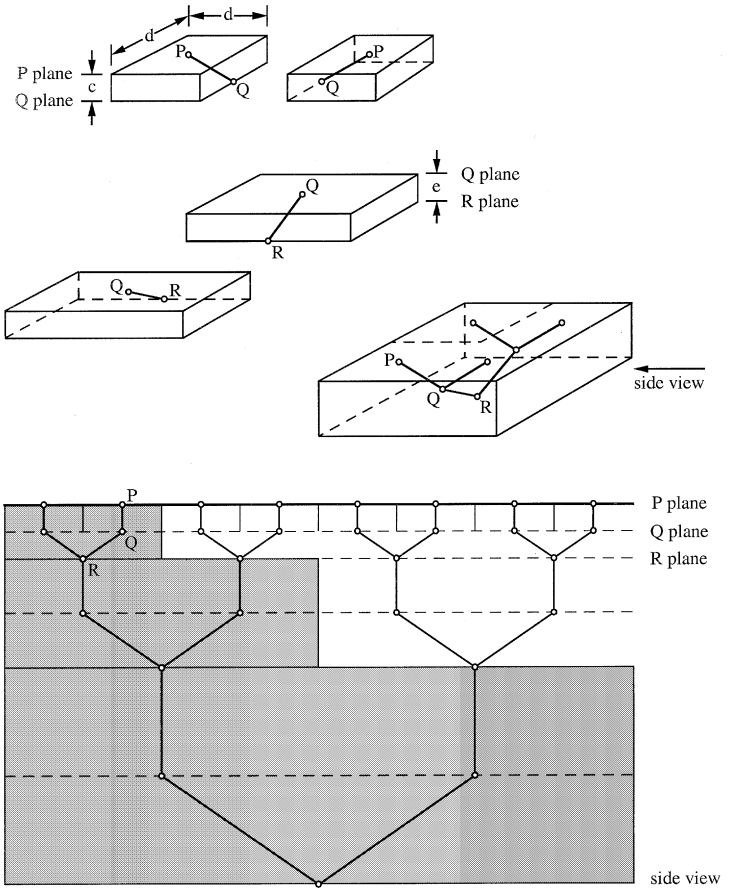

Fig. 2. The construction of the minimal-length tree between a plane and a point, and a side view of the tree-shaped path.

$d \times d$), which started the construction. The construction continues toward planes situated successively under plane R, and the steps are the same two steps that we outlined, from P to Q, and from Q to R. This sequence is indicated by the side view of the construct, which is shown in the lower part of Fig. 2.

4. Tree between a circle and its center

In the preceding two sections we relied on a single idea, and we developed two tree-shaped structures, one in the plane (Fig. 1) and the other in the three dimensional space (Fig. 2). The idea is that in an elemental rectangle such as $c \times d$ (Fig. 1) there exists an optimal rectangle shape (c/d) such that the "path out of the rectangle" is the shortest. The power of an idea comes from its generality. In this section and the next we show that the same shape-optimization opportunity can be used to derive minimal-length flow paths for considerably more complicated configurations.

In Fig. 3 we propose to construct the connection between the points of a circle and the center of the circle. This configuration is similar to taking the point–line structure of Fig. 1, and curving the P line around point S, so that S becomes the center of a circle. The rectangular building blocks used in Fig. 1 become deformed (curvilinear) rectangles. The deformed rectangle is closer to a true rectangle if it is far from the center. The degree of closeness is associated with the distance (r) between the rectangular element and the center.

Consider the elemental curvilinear rectangle of radial distance r, angle θ, and radial thickness δ, which is shown in the upper part of Fig. 3. The area of this element is fixed,

$$A = \frac{1}{2}\theta(2r\delta - \delta^2), \quad \text{constant.} \tag{3}$$

The role of segment PQ of Fig. 1 is played by segment l. The objective is to minimize l subject to constraint (3), i.e., to minimize

$$l^2 = a^2 + b^2 = \left[r\left(1 - \cos\frac{\theta}{2}\right) + \delta\cos\frac{\theta}{2}\right]^2 + (r-\delta)^2 \sin^2\frac{\theta}{2}. \tag{4}$$

It is convenient to nondimensionalize Eqs. (4) and (3) by using r as length scale,

$$\left(\frac{l}{r}\right)^2 = (1-x)^2 - 2(1-x)\cos\frac{\theta}{2} + 1, \tag{5}$$

$$\frac{A}{r^2} = \frac{\theta}{2}(2x - x^2), \tag{6}$$

where $x = \delta/r$. According to the method of Lagrange multipliers [14], the problem of finding the extremum of function (5) subject to constraint (6) is equivalent to finding the extremum of the aggregate function

$$\Phi = (1-x)^2 - 2(1-x)\cos\frac{\theta}{2} + 1 + \lambda\theta\left(x - \frac{1}{2}x^2\right). \tag{7}$$

Solving the system $\partial\Phi/\partial x = 0$ and $\partial\Phi/\partial\theta = 0$, and eliminating the Lagrange multiplier λ, we obtain the relation that pinpoints the optimal aspect ratio of the curvilinear rectangle:

$$\frac{x}{\theta} = \frac{(1-x)^2 \sin\frac{\theta}{2}}{(2-x)\left(x - 1 + \cos\frac{\theta}{2}\right)}. \tag{8}$$

To see how Eq. (8) leads us to optimal shapes, and later to point–circle trees, assume that $\theta \ll 1$, such that $\cos(\theta/2) \cong 1$ and $\sin\theta/2 \cong \theta/2$. Eq. (8) becomes

$$\frac{x}{\theta} \cong \frac{1-x}{2^{1/2}(2-x)^{1/2}}, \tag{9}$$

where x/θ is the aspect ratio of the curvilinear rectangle, $x/\theta = \delta/(r\theta)$. When the radial dimension of the

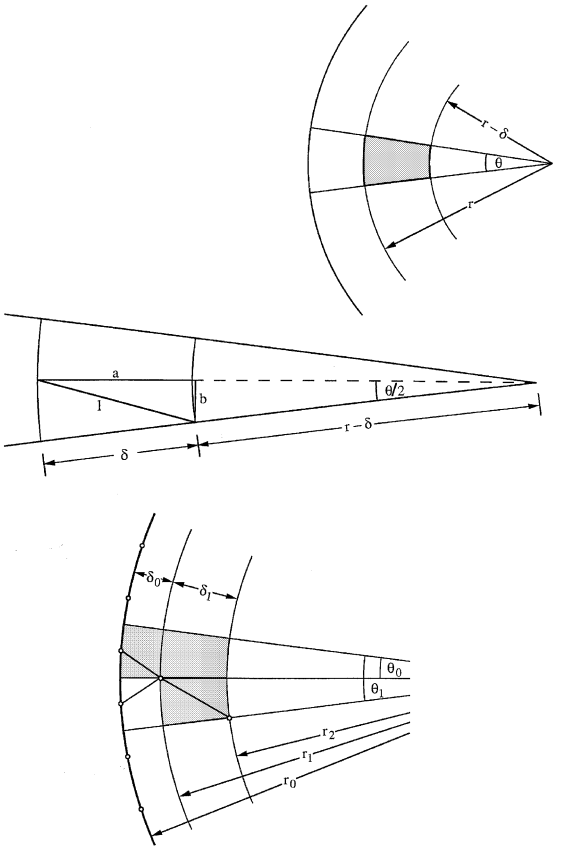

Fig. 3. Curvilinear rectangle defined by the intersection of radial lines and concentric circles, and the construction of the minimal-length tree between a circle and its center.

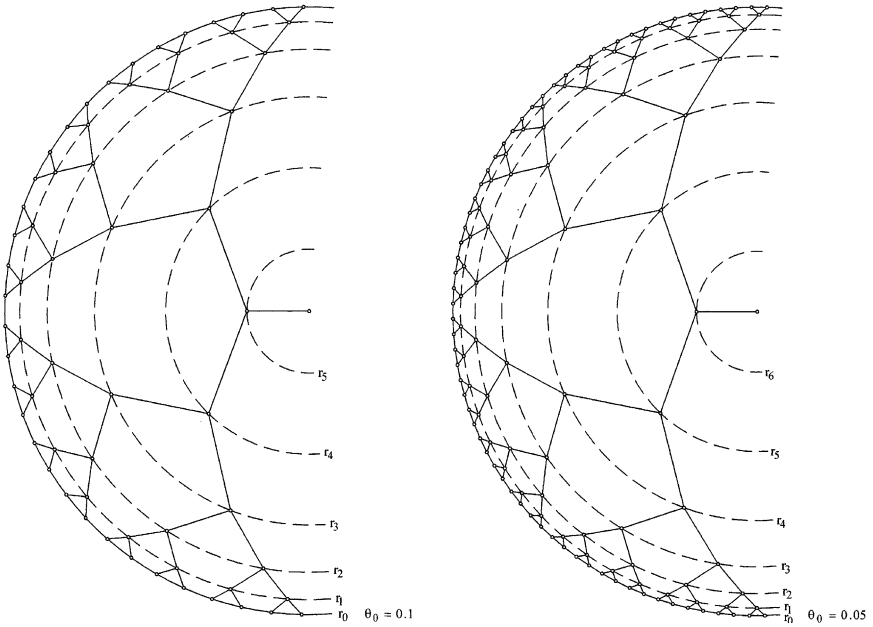

Fig. 4. Examples of tree-shaped connections between a circle and its center. The θ_0 value accounts for the number of points on the circle.

rectangle (δ) is small in comparison with its distance to the center (r), i.e., when $x \ll 1$, the optimal aspect ratio is $\delta/(r\theta) \cong 1/2$, in accordance with Section 2. Closer to the center of the circle, where x is progressively larger, the optimal aspect ratio is progressively greater than 1/2. We can expect the same trends from the exact solution, Eq. (8).

To construct the minimal-length path between the outer circle (radius r_0) and the center (O), we start from the outer circle and approximate it as a string of equidistant points (P). See the lower part of Fig. 3. The distance between two consecutive points is d. The angle sustained by the outermost (elemental) rectangle of peripheral length d is $\theta_0 = d/r_0 \ll 1$. The value of θ_0 must be selected at the start of construction, e.g., $\theta_0 = 0.1$. Substituting θ_0 for θ in Eq. (8), we calculate x_0, or the aspect ratio of the elemental rectangle (x_0/δ_0), or the radial thickness of the element, $\delta_0 = r_0 x_0$. The radius of the inner circle that borders the elemental rectangle is $r_1 = r_0 - \delta_0$.

The next curvilinear rectangle subtends the angle $\theta_1 = 2\theta_0$, and has the radial position r_1. Eq. (8) delivers x_1, the aspect ratio x_1/δ_1, and the radial dimension $\delta_1 = r_1 x_1$. The radius of the next circle is $r_2 = r_1 - \delta_1$.

This algorithm can be applied a sufficient number of times, marching toward the center of the circle, and drawing the resulting tree network. The construction must stop at a certain step (i) if

$$\theta_i > 2\pi \tag{10}$$

or

$$r_i < 0 \tag{11}$$

whichever occurs first. During the numerical implementation of the algorithm we found that thresholds (10) and (11) are reached simultaneously in this construction. The constructions for $\theta_0 = 0.1$ and $\theta_0 = 0.05$ are reported in Fig. 4. We expect the constructed tree to be imperfect approximate near the center, because the rectangle approximation becomes poorer in the limit $r \to 0$.

5. Tree between one point and many points distributed uniformly over an area

In the preceding sections we constructed minimum-length paths for connecting one point source (or sink) to a large number of point sinks (or sources) situated on a line, or on a plane. In the case of the plane, the point source S was situated at a distance away from the plane (Fig. 1). The space between the point source and the plane did not contain any sources or sinks – it contained the connecting network.

In this section we consider the more challenging problem of connecting the point source to a large number of point sinks that cover an area uniformly. The point source and the many sinks are in the same plane. We may think of this configuration as a river basin (the area) that collects rain water at a uniform rate per unit

area, and which uses its links (rivulets and rivers) to channel the collected water out of the territory, as a single stream. We may also think of this problem as a modification of the line–point flow network of Fig. 1, where the added feature is the presence of uniformly distributed points (sources, or sinks) on the area between the P line and the common source or sink (S).

How the construction starts depends on how the points are distributed over the given area. The simplest construction is sketched at the top of Fig. 5, where the assumption is that the points are distributed in a square pattern. The start is the elemental area of size A_0, which is allocated to one of the many points P. By performing a length-minimization analysis that is analogous to the analysis of Section 2, we find that the shape of A_0 must be square. In this case the distance from P to the corner of A_0 (the exit from the elemental area) is the shortest. The side of the elemental square is $L_0 = A_0^{1/2}$.

Square elements can be assembled tightly into square constructs of progressively larger sizes. Each new construct, A_i, consists of four constructs of the preceding size, $A_i = 4A_{i-1} = 4^i A_0$ $(i = 1, 2, \ldots)$. The first construct (A_1, Fig. 5) has the purpose of connecting four points (P_1, P_2, P_3, P_4) to the single exit point Q. The way out of area A_1 is a cross in which three half-diagonals meet in the center of A_1, and the stem touches point P_4 before reaching Q. In the drawing of A_1 we have employed lines of increasing thicknesses, to suggest that elemental streams combine into larger streams en route to the exit (Q).

The second construct is itself a cross-shaped assembly of first constructs. Fig. 5 shows that the exit points of

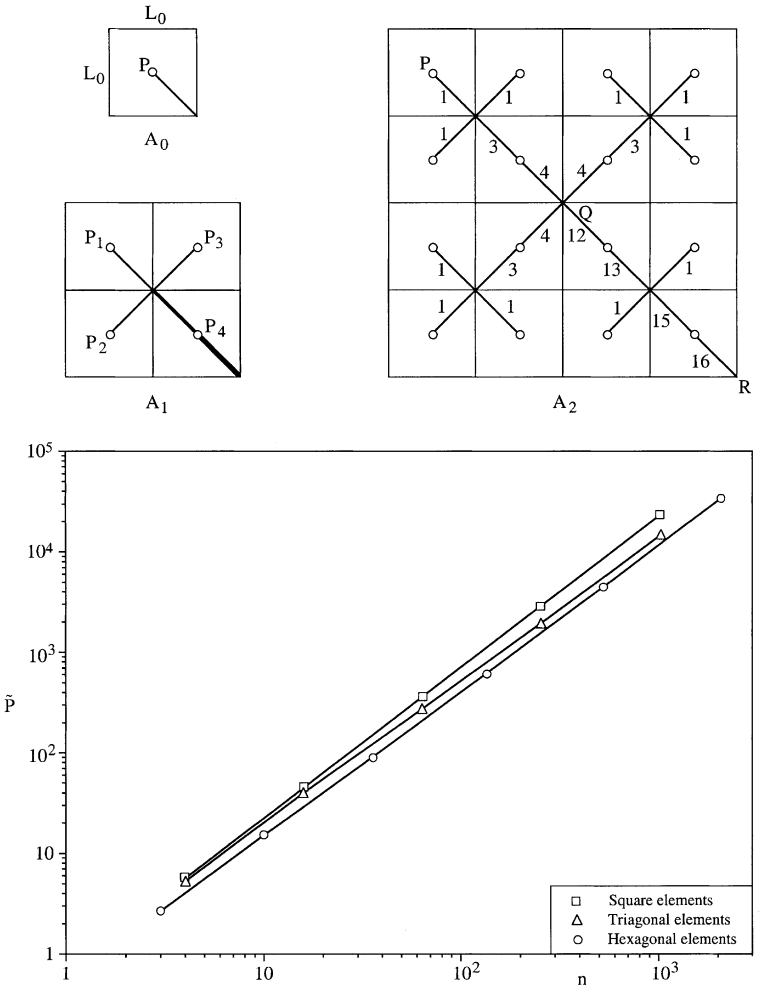

Fig. 5. Top: The construction of the tree between one point (R) and an area covered uniformly by points (P) arranged in a square pattern. Bottom: The overall flow resistance between the point (source, sink) and the most distant point of the area that is covered uniformly with points.

three A_1-size constructs meet in the Q center of the second construct. The fourth A_1 construct is connected to the network, as the diagonal stem travels from Q to R. The flow rate increases in steps, from P to R. The numbers attached to each link indicate the relative magnitude of each local flow rate, where "1" stands for the flow rate that reaches each elemental point of type P.

As figure of merit for the resulting tree network we evaluate the pressure difference between the farthest point on the territory (e.g., point P on A_2) and the exit point (point R on A_2). For simplicity, we assume that all the pipes have the same diameter, and the flow is in the Hagen–Poiseuille regime through every pipe. The pressure drop across one link (ΔP_k) is proportional to the mass flow rate through the link ($\dot{m}_k$) and the length of the link (L_k). The mass flow rate changes from one link to the next, where L_k is constant and equal to the half-diagonal of the elemental square, $L_k = 2^{-1/2}A_0^{1/2}$. If $\dot{m}_0$ is the mass flow rate through one elemental link (the link that touches point P), then the ratio $\dot{m}_k/\dot{m}_0$ is the relative flow rate indicated by the number attached to each link of the A_2 construct in Fig. 5. To summarize, the pressure drop across link k is

$$\Delta P_k = C\dot{m}_k L_k, \tag{12}$$

where the C coefficient is a constant dictated by the kinematic viscosity of the fluid and the pipe diameter D, namely $C = 128\nu/(\pi D^4)$. The pressure drop from the most distant point P (the upper-left corner of A_2) to the exit point (e.g., R of A_2) is obtained by summing along the descending diagonal the link pressure drop contributions ΔP_k,

$$\Delta P = \sum_{\text{from P, to Q,R,...}} \Delta P_k. \tag{13}$$

This quantity can be nondimensionalized as

$$\tilde{P} = \frac{\Delta P}{C\dot{m}_0 A_0^{1/2}} \underset{\text{Q}}{} \underset{\text{R}}{} \underset{\text{S}}{} = 2^{-1/2}(1 + 3 + 4 + 12 + 13 + 15 + 16 + 48 + \cdots + 64 + \cdots), \tag{14}$$

where the numbers in the brackets represent the relative mass flow rates through the links of the descending diagonal. The pressure drop increases stepwise as the size of the construct increases. The latter is also indicated in Eq. (14) by the label of the exit corner of each construct $(\text{Q}, \text{R}, \ldots)$, which is placed above the relative flow rate of the stream that leaves through the lower-right corner of each construct $(4, 16, 64, \ldots)$. The way in which the overall pressure drop increases as the covered territory grows is indicated by square symbols in the lower part of Fig. 5, where n is the number of elements of size A_0 contained in the total area covered by the construct.

Another way to cover an area uniformly with points is to assign an approximately round area A_0 to each point, and to fit the A_0 elements so that they cover the given territory completely. A tight packing is obtained when each A_0 is squeezed into the shape of a regular hexagon with $L_0 = bA_0^{1/2}$ as the distance between the opposing sides of the hexagon, $b = (2/3)^{1/2}(\tan 30°)^{-1/2}$. The point P is the center of the hexagon, as shown in the first drawing of Fig. 6. The path out of the element is the line of length $L_0/2$, from P to the midpoint of one side of the hexagon. This packing places the points of type P into a pattern of equilateral triangles.

The construction sequence is described in Fig. 6. The first construct consists of only three elements. The distance between adjacent points is L_0. The three points are connected by an asymmetric Y-shaped path with the root at the exit Q. We find that asymmetry is a necessary feature of assembly when the A_0 elements are the roundest, i.e., regular hexagons. Asymmetry distinguishes the tree-shaped paths of Fig. 6 from the trees connecting square constructs (Fig. 5). Dichotomy, or pairing of two links to form a stem is another feature that distinguishes Fig. 6 from Fig. 5.

The second construct (A_2) brings to light another feature that was not present in Fig. 5. A hole of size A_0 is left uncovered when first constructs are assembled into a second construct. In Fig. 6 the hole is in the center of A_2, and is covered by one A_0 element (shown darker). The drawing also shows the relative mass flow rates along each link. Asymmetry is accentuated at the second-construct level, because the central A_0 element must be connected to one of the two sides of the large V that contains the tree network. The flow rates collected by the two sides of the V are slightly unbalanced (5, vs. 4 mass flow rate units), as they reach the center of the bottom element. We will show that minimizing this imbalance is important from the point of view of optimizing the network, i.e., for the purpose of distributing the imperfections of the network optimally.

These distinguishing features are even more striking in larger constructs. The first drawing in the bottom row of Fig. 6 shows how a third construct can be formed by assembling three second constructs. A hole of size $6A_0$ is left uncovered in the middle of the third construct. The central part of this hole was filled with one first construct, which is dark. The remaining corners of the hole (lighter shadow) are connected to the nearest points. The numbers indicate the relative mass flow rate through each link. Asymmetry and flow imbalance are evident. The two branches of the large V, which meet at the bottom of the third construct, show a flow rate imbalance of 20 units versus 15.

In addition to asymmetry and imbalance, in Fig. 6 we see the emergence of increasingly more freedom in how to connect the elements of the inner hole to the structure that delineates each new V-shaped construct. The rule of

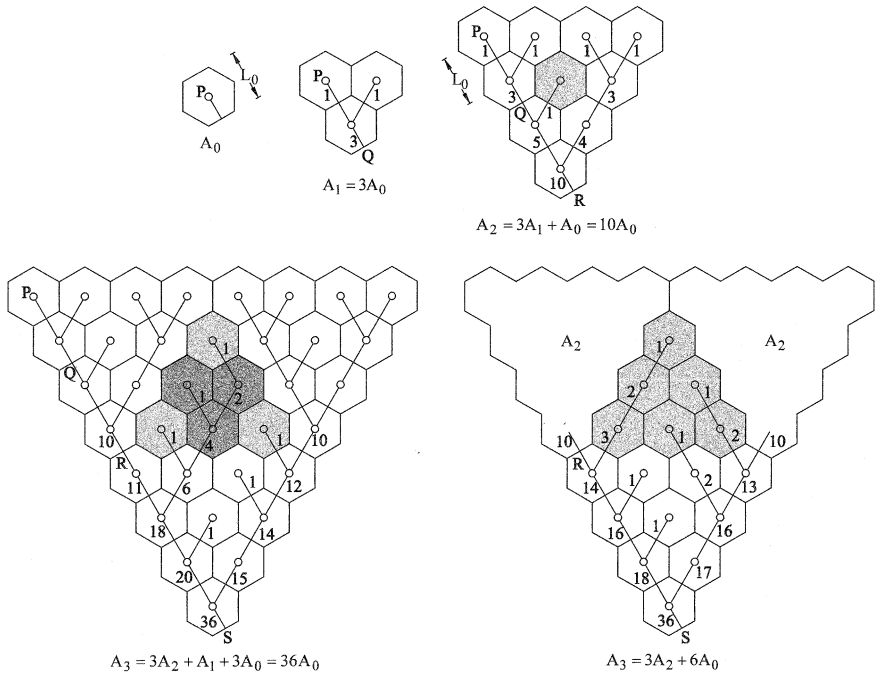

Fig. 6. The construction of the tree between one point (Q, R, ...) and an area covered uniformly by hexagonal area elements. The bottom row shows two designs for covering the central area of the third construct.

assembly applied from A_0 to A_1, from A_1 to A_2, from A_2 to A_3, etc., concerns only the corner areas of each triangular construct. The new construct is made of three constructs of the preceding size, plus filler area in the middle. There is more than one way of connecting the central area to the peripheral building blocks of the structure. The lower-left drawing of Fig. 6 shows one way. Better ways can be found by analyzing the performance of the tree-shaped flow network.

The calculation of the overall pressure drop between P and subsequent exit points (Q, R, S, ...) in Fig. 6 follows the steps described in conjunction with Eqs. (12)–(14). We employ the same notation, and assume that the elemental area A_0 of Fig. 6 is the same as the area A_0 of Fig. 5. This means that the length scale L_0 of Fig. 6 is not exactly the same as the L_0 scale of Fig. 5. With reference to the left side of the V-shaped A_3 construct shown in the lower-left drawing of Fig. 6, the overall pressure drop is

$$\tilde{P} = \frac{\Delta P}{C\dot{m}_0 A_0^{1/2}} \overset{Q}{} \overset{R}{} \overset{S}{} = b\left(1 + 3 + 5 + 10 + 11 + 18 + 20 + \frac{1}{2}36 \cdots\cdots\right). \quad (15)$$

A smaller $\tilde{P}$ value is found if the calculation proceeds along the right side of the V,

$$\tilde{P} = b(1 + 3 + 5 + 10 + 12 + 14 + 15 + \frac{1}{2}36 \cdots). \quad (16)$$

The higher $\tilde{P}$ value prevails, and measures the overall imperfection (resistance) of the flow path. Clearly, a smaller-flow rate at the root of the side along which $\tilde{P}$ is calculated is good for the purpose of decreasing $\tilde{P}$. A smaller flow rate is achieved by balancing as closely as possible the two sides of each V. The lower-right drawing of Fig. 6 shows a more balanced way of connecting the inner hole (dark) to the three A_2 constructs that make up A_3. The flow imbalance at the bottom of the V is 18 units versus 17. The overall pressure drop along the left side of the V is

$$\tilde{P} = b\left(1 + 3 + 5 + 10 + 14 + 16 + 18 + \frac{1}{2}36 \cdots\right), \quad (17)$$

which is less than in Eq. (15). Balancing resistances, or optimizing the distribution of imperfection is effective [1].

The $\tilde{P}$ values calculated based on Fig. 6 (lower right) and Eq. (17) are plotted versus n in Fig. 5, where n is the number of A_0 elements in each construct. These points are indicated by circles, and fall below the apparent line of squares associated with the upper part of Fig. 5. The conclusion is that the construction of Fig. 6 is more effective for the purpose of connecting one point to the

large number of points distributed uniformly over an area.

To see even more clearly why the assembly of regular hexagons is a more effective flow structure, consider the only option that is still available for covering an area with elements that are regular polygons. That option is to use elements shaped as equilateral triangles, Fig. 7. The elemental area A_0 is the same as in the case of square elements (Fig. 5) and hexagonal elements (Fig. 6). Fig. 7 shows that when a large area is covered by equilateral triangles, the centers of mass of the triangles (P) arrange themselves in a pattern of regular hexagons. The side of the hexagon, or the shortest distance between two points of type P is $L_0 = b' A_0^{1/2}$, where $b' = (2/3)(\tan 30°)^{-1/2}$. The length L_0 is not the same as the L_0 dimensions used earlier.

Fig. 7 shows the first steps in the construction based on equilateral triangles. The first construct (A_1) consists of four elements, and is itself an equilateral triangle. The four center points (P) are linked into a symmetric Y-shaped flow path. The exit from the first construct (Q) is along the shortest path from the Y structure to the boundary of A_1. The number attached to each link indicates the relative flow rate, where 1 represents the elemental flow rate arriving at or departing from a center point P.

The second construct (A_2) is formed by three A_1 constructs and an inner area of size $4A_0$. The A_2 drawing

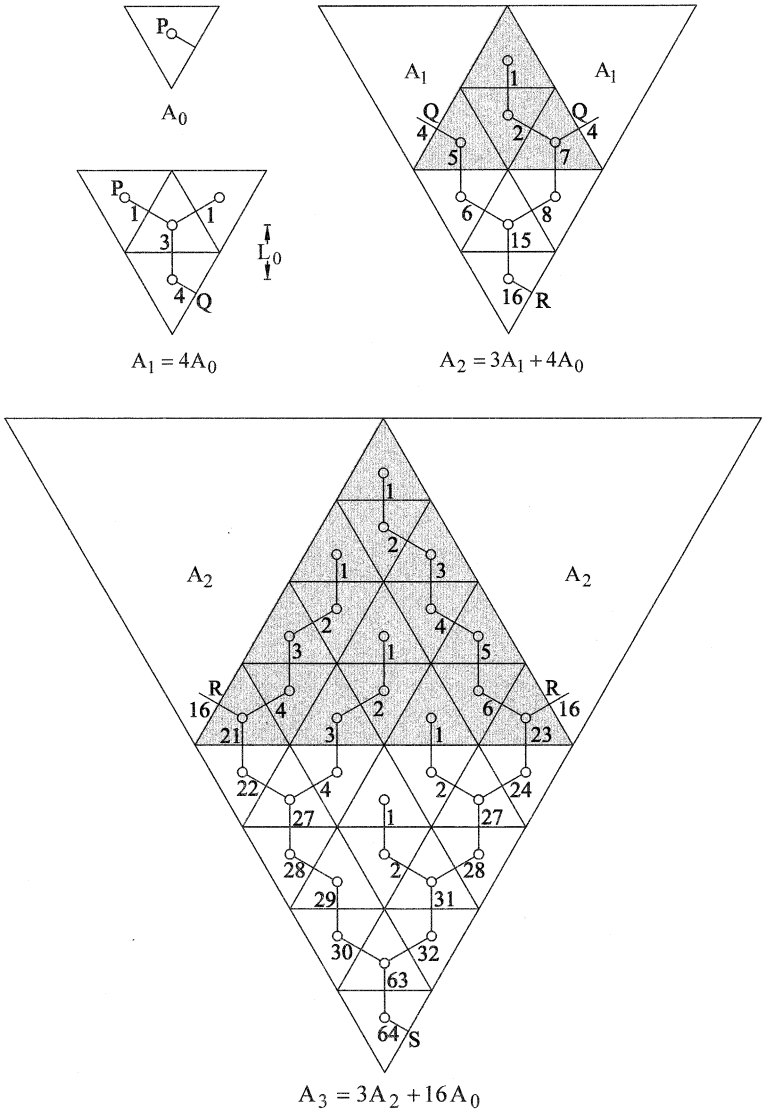

Fig. 7. The construction of the tree between one point (Q, R, ...) and an area covered by area elements shaped as equilateral triangles.

shows the only way in which the centers of the four inner elements can be connected to the rest of the network, so that the resulting flow structure is without loops. The result is asymmetry: Note the asymmetric connections that cover the shaded area. Note also the flow rate imbalance (5 vs. 7) between the streams that enter the bottom A_1 construct. The construction of Fig. 7 can be extended to cover larger areas, as shown by the A_3 design.

The performance of the structure based on triangular elements can be evaluated by using the same pressure drop model and calculation procedure as in Eqs. (14) and (17). For the structure of Fig. 7 we obtain

$$\tilde{P} = \frac{\Delta P}{C\dot{m}_0 A_0^{1/2}} \qquad \begin{matrix} \text{Q} \\ \\ \end{matrix} \qquad \begin{matrix} \text{R} \\ \\ \end{matrix}$$
$$= b'\left(1 + 3 + \frac{1}{2}4 + \frac{1}{2}4 + 7 + 8 + 15 + \frac{1}{2}16 + \frac{1}{2}16 + \cdots\right). \tag{18}$$

Note the relative flow rate indicated by 7 in the fifth term inside the round brackets. This means that at the A_2 level we chose to estimate the largest pressure drop, which occurs between the extremities of the upper-right A_1 area and the root R. Had we chosen the upper-left A_1 construct as the start of the ΔP calculation, we would have used 5 in place of 7, and we would have underestimated the actual overall pressure difference sustained by the second construct.

The $\tilde{P}$ values generated based on Fig. 7 and Eq. (18) are indicated by triangles in Fig. 5. These values fall between the preceding two sets (squares, circles), and reconfirm the conclusion that the most effective flow structure is the one based on hexagonal elements. Structures with hexagonal and triangular elements perform nearly the same as their complexity (n) increases. They perform better than structures with square elements, and this suggests that structures with pairings perform better than structures with three tributaries at each point of confluence.

There is another geometric conclusion that we must stress, and it refers to the angles between branches. From triangular area elements, to square and hexagonal elements, the angles decrease from 120° to 90° and 60°. The smallest angle corresponds to the best structure, and it comes from "packing" needs – how to cover an area completely by using the shortest links between the centers of elements. The 60° angle of confluence or branching, which looks so much like the natural angles of the trees known from physiology and geophysics, is a consequence of packing, or the difficulty of covering an area with identical elements. In this paper, the 60° angle does not come from an optimization procedure such as the minimization of flow resistance at the level of one pairing or bifurcation, as reported earlier by Zamir [15], Ledezma et al. [16] and Bejan et al. [11].

6. Three-dimensional trees

The selection of flow problems in this paper followed an exploratory course, from the simple toward the complex. Most of the work referred to tree-shaped connections in a plane, because flat trees are relatively simpler and easier to illustrate on paper. Their importance in practice remains undiminished, in view of the many natural trees found in river basins, vascularized membranes, traffic patterns and power distribution networks.

The direction of future work is to extend the present construction method to trees in three dimensions, to connect one point to many points distributed uniformly through a volume. We made a step in this direction in Section 3, where the connection was between the many points of a plane and one point situated off the plane (Fig. 2). The next challenge is to consider the case where the entire space around the single point (S) is populated uniformly by points that must be connected optimally to S. This extension is beyond the scope of this study, and is proposed for future work.

A basic question is whether the best Y-shaped assemblies of two links joined into one link are flat or three-dimensional. The example of by Fig. 2 is one where the Y construct lies in two planes that intersect at an angle. Two branches of type PQ form a plane, while the stem QR pierces that plane at an angle. Is a perfectly flat Y construct better? This question is relevant, because careful observations of three-dimensional branchings in the cardiovascular tissue have indicated conclusively that the flat Y construct is the prevailing form in three-dimensional trees [17].

Consider the two bent-Y constructs obtained in the first two stages of Fig. 2. The volume occupied by one such construct is the same as that of the smallest shaded rectangle in the upper-left corner of Fig. 3. We consider this volume fixed, $V = 2d^2(c + e)$ or $V = 2^{1/2}d^3$, because $c = e = 2^{-3/2}d$. The bent Y structure has two lengths, $\overline{\text{PQ}} = L_0 = (c^2 + d^2/4)^{1/2} = (3/2)^{1/2}d/2$, and $\overline{\text{QR}} = L_1 = (e^2 + d^2/4)^{1/2} = L_0$. In order to evaluate the performance of this structure as a path of least flow resistance, we assume that the Y is the confluence of two round tubes of diameter D_0 and length L_0, which form one tube of diameter D_1 and length L_1. We assume that the total tube volume is constrained, $V_t = 2(\pi D_0^2/4)\times L_0 + (\pi D_1^2/4)L_1$, that the flow is in the Hagen–Poiseuille regime, and that the ratio of tube diameters has been optimized for minimal resistance, $D_1/\ D_0 = 2^{1/3}$. Using this ratio and $L_0 = L_1$, we rewrite the tube volume constraint as $V_t = (\pi/2)(1 + 2^{-1/3})D_0^2 L_0$. The pressure drop across the Y structure is $\Delta P = \Delta P_1 + \Delta P_0$, where ΔP_1 and

ΔP_0 are the pressure drops across the L_1 tube (flow rate $\dot{m}$) and, respectively, across the L_0 tube (flow rate $\dot{m}/2$),

$$\Delta P = C'\dot{m}\frac{L_1}{D_1^4} + C'\frac{\dot{m}}{2}\frac{L_0}{D_0^4}, \tag{19}$$

where $C' = 128v/\pi$. Eq. (19) can be nondimensionalized into an overall flow resistance, after using the preceding results for L_0, L_1 and D_1/D_0, and by eliminating D_0 and d between Eq. (19) and the V and V_t constraints:

$$\tilde{P}_{\text{bent Y}} = \frac{\Delta P V_t^2}{\dot{m} C' V} = \frac{3^{3/2}\pi^2}{2^8}(1 + 2^{-1/3})^3 = 1.156. \tag{20}$$

The analysis and optimization of the flat Y structure is performed in relation to the drawing shown in Fig. 8. The Y structure lies in the plane of size $f \times 2d$. The volume inhabited by the construct has the same size as before, $V = 2d^2 g$. The height of the rectangle in which the Y structure resides is $f = (g^2 + d^2/4)^{1/2}$. The inclination of this plane is free to change, and so is the length L_1, or the location of the Q junction. In summary, the Y-shaped construct has two degrees of freedom, which in the following analysis are represented by the aspect ratios a/d (or L_0/L_1) and f/d, where $a = f - L_1$. The overall pressure drop, Eq. (19), can be combined with the V_t constraint and $D_1/D_0 = 2^{1/3}$, and the result is

$$\Delta P = \frac{\dot{m} C' \pi^2}{8 V_t^2}(L_0 + 2^{-1/3} L_1)^3. \tag{21}$$

The group in the round brackets can be minimized by varying the geometry. We accomplish this in two steps. First, we assume that the rectangular area $f \times (2d)$ does not change. On it, the only variable is a, or the position of point Q. The group $(L_0 + 2^{-1/3}L_1)$ can be expressed as a function of a, f and d, and can be minimized with respect to a. The result is the optimal ratio $a/d = c_a$, where $c_a = 2^{-1}(2^{2/3} - 1)^{-1/2}$. Related results are $L_0/d = c_0$, where $c_0 = (1 - 2^{-2/3})^{-1/2}/2$, and $L_1/d = f/d - c_a$. These values can be substituted into Eq. (21), and after eliminating d^3 based on the V constraint, we obtain the dimensionless flow resistance of the flat Y construct:

$$\tilde{P}_{\text{flat}} = \frac{\pi^2[c_0 + 2^{-1/3}(f/d - c_a)]^3}{16[(f/d)^2 - 1/4]^{1/2}}. \tag{22}$$

We found numerically that this function reaches its minimum at $f/d = 0.716$, where its value is $\tilde{P}_{\text{flat Y}} = 0.800$. Other relevant geometric characteristics of the optimized structure are $a/d = 0.652$, $g/d = 0.512$, $L_0/L_1 = 13.01$ and $L_1/f = 0.088$.

Eqs. (20) and (22) show that the global resistance of the flat Y structure is 30 percent smaller than the global resistance of the bent Y structure. This lends support to the view [1] that natural Y structures, which are flat [17], are results of a process of flow access optimization.

7. Concluding remarks

In this paper we explored a simpler and more direct route to the construction of tree-shaped flow structures connecting discrete points (sources, sinks) with large numbers of points (lines, areas, volumes). The starting point was the observation that the shape of an elemental volume of the flow network can be selected such that the length of the flow path housed by the element is minimal. By proceeding toward larger and more complex structures (elements, first constructs, second constructs, ...), we constructed flow networks between one point and a straight line (Section 2), one point and a plane (Section 3), a circle and its center (Section 4), and one point and many points distributed over an area (Section 5). In the latter we also considered a specific example of laminar fluid flow through a network with tubes of the same diameter, and showed that tube lengths and the shape of the interstitial area elements govern the optimization of the flow architecture.

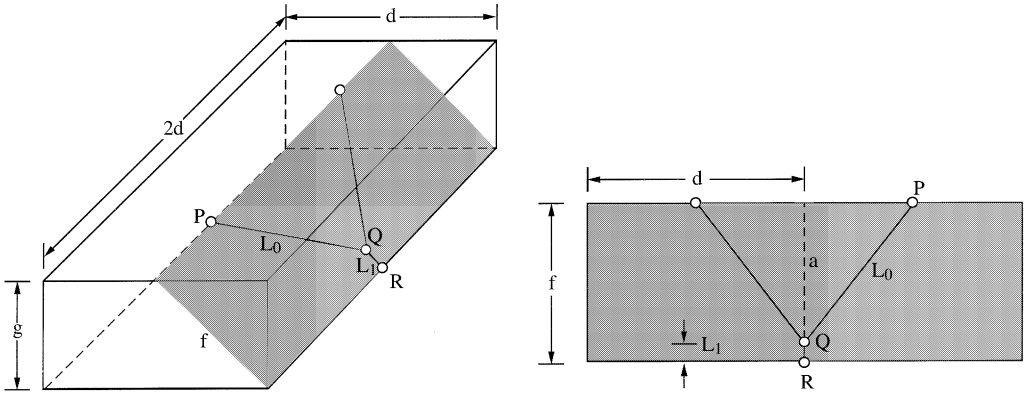

Fig. 8. Flat Y-shaped flow construct in the elemental volume of a three-dimensional tree network.

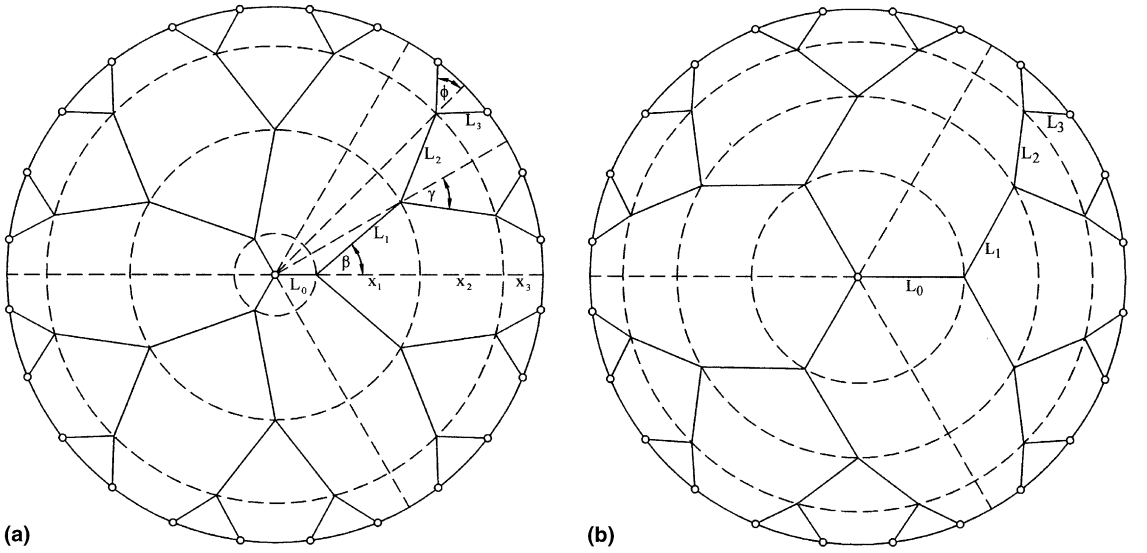

Fig. 9. Tree flows between a circle and its center: (a) construct obtained by optimizing every geometric detail; and (b) construct produced by the length-minimization algorithm presented in Section 4.

To evaluate the effectiveness of the minimal-length structures developed in this paper, we compared the point–circle construction of Section 4 with a tree-shaped network obtained by optimizing every geometric detail of the flow network. The optimization of every detail is reported in [18]. The comparison is made on a common basis: the circle of fixed radius r_0, the use of tube pairing, and the fixed total volume of the tubes with Hagen–Poiseuille flow, V_t. The step change in tube diameters is optimized in accordance with Eq. (1). The number of points arranged equidistantly on the circle is $N = 24$.

Fig. 9(a) shows the flow structure derived after optimizing features such as L_0, L_1, L_2, L_3, β, γ, ϕ, x_1, x_2 and x_3, where $r_0 = L_0 + x_1 + x_2 + x_3$. The overall flow resistance is [18]

$$\frac{\Delta P}{\dot{m}} = 8\pi\nu\frac{r_0^3}{V_t^2}f, \tag{23}$$

where ΔP is the pressure difference between the center and the circle, $\dot{m}$ is the total mass flow rate, f is the dimensionless flow resistance

$$f = n_0\left(\sum_{j=0}^{p} 2^{j/3}\frac{L_j}{r_0}\right)^3, \tag{24}$$

where n_0 is the number of tubes that reach the center ($n_0 = 3$), and p is the number of levels of pairing

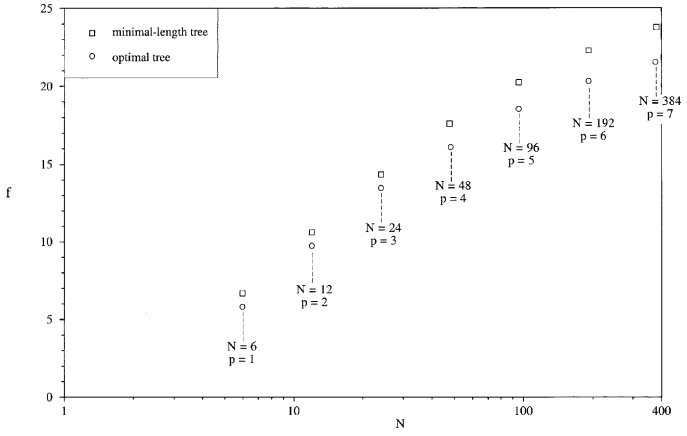

Fig. 10. The global flow resistance for: (a) constructs obtained by optimizing every geometric detail; and (b) constructs produced by the length-minimization algorithm presented in Section 4.

($N = 3 \times 2^P$). The structure of Fig. 9(a) is the result of minimizing f by exploiting all the degrees of freedom of the flow architecture. The minimized f value is plotted in Fig. 10 not only for $N = 24$ but also for other numbers of points on the circular perimeter (N).

Fig. 9(b) shows the corresponding structure designed based on the length-minimization algorithm developed in Section 4. Visually, there is relatively little difference between the two constructions, Figs. 9(b) and (a). The same can be said about the f values of the competing designs. The squares plotted on Fig. 10 show that, although consistently inferior, the performance of minimal-length structures resembles closely the performance of fully optimized structures. In conclusion, the length-minimization method proposed in this paper provides a very effective shortcut to designs that come close to the best designs. The minimal-length designs approach the optimal designs in terms of global performance, and architecturally as well. The closeness documented in Figs. 9 and 10 shows again that optimized tree flow structures are robust [1].

Acknowledgements

This work was supported in part by the National Science Foundation and King Mongkut's University of Technology (KMUTT), Thailand.

References

[1] A. Bejan, Shape and Structure, from Engineering to Nature, Cambridge University Press, Cambridge, UK, 2000.
[2] D'A.W. Thompson, On Growth and Form, Cambridge University Press, Cambridge, UK, 1942.
[3] E.R. Weibel, Morphometry of the Human Lung, Academic Press, New York, 1963.
[4] K. Schmidt-Nielsen, Scaling: Why is Animal Size so Important? Cambridge University Press, Cambridge, UK, 1984.
[5] S. Vogel, Life's Devices, Princeton University Press, Princeton, NJ, 1988.
[6] S.A. Schumm, M.P. Mosley, W.E. Weaver, Experimental Fluvial Geomorphology, Wiley, New York, 1987.
[7] N. MacDonald, Trees and Networks in Biological Models, Wiley, Chichester, 1984.
[8] H.L. Willis, W.G. Scott, Distributed Power Generation: Planning and Evaluation, Marcel Dekker, New York, 2000.
[9] C.D. Murray, The physiological principle of minimal work in the vascular system, and the cost of blood-volume, Proc. Acad. Natl. Sci. 12 (1926) 207–214.
[10] T.A. Wilson, Design of the bronchial tree, Nature (London) 213 (1967) 668–669.
[11] A. Bejan, L.A.O. Rocha, S. Lorente, Thermodynamic optimization of geometry: T- and Y-shaped constructs of fluid streams, Int. J. Therm. Sci. 39 (2000) 949–960.
[12] C.D. Murray, The physiological principle of minimum work applied to the angle of branching of arteries, J. Gen. Physiol. 9 (1926) 835–841.
[13] A. Lösch, The Economics of Location, Yale University Press, New Haven, CT, 1954.
[14] K. Rektorys (Ed.), Survey of Applicable Mathematics, The MIT Press, Cambridge, MA, 1969, pp. 480–484.
[15] M. Zamir, Cost of departure from optimality in arterial branching, J. Theor. Biol. 109 (1984) 401–409.
[16] G.A. Ledezma, A. Bejan, M.R. Errera, Constructal tree networks for heat transfer, J. Appl. Phys. 82 (1997) 89–100.
[17] M. Zamir, Arterial bifurcations in the cardiovascular system of a rat, J. Gen. Physiol. 81 (1983) 325–335.
[18] W. Wechsatol, S. Lorente, A. Bejan, Optimal tree-shaped networks for fluid flow in a disc-shaped body, Int. J. Heat Mass Transfer 45 (2001), submitted.